

## Unconventional Ferromagnetic and Spin-Glass States of the Reentrant Spin Glass $\text{Fe}_{0.7}\text{Al}_{0.3}$

Wei Bao,<sup>1,2</sup> S. Raymond,<sup>1,3</sup> S. M. Shapiro,<sup>1</sup> K. Motoya,<sup>4</sup> B. Fåk,<sup>3</sup> and R. W. Erwin<sup>5</sup>

<sup>1</sup>Brookhaven National Laboratory, Upton, New York 11973

<sup>2</sup>Los Alamos National Laboratory, Los Alamos, New Mexico 87545

<sup>3</sup>CEA-Grenoble, DRFMC-SPSMS, 38054 Grenoble Cedex 9, France

<sup>4</sup>Science University of Tokyo, Noda 278, Japan

<sup>5</sup>National Institute of Standards and Technology, Gaithersburg, Maryland 20899

(Received 19 October 1998)

Spin excitations in a single crystal of  $\text{Fe}_{0.7}\text{Al}_{0.3}$  were investigated over a wide range of energy and reciprocal space with inelastic neutron scattering. In the ferromagnetic phase, propagating spin wave modes become paramagnonlike diffusive modes beyond a critical wave vector  $\mathbf{q}_0$ , indicating substantial disorder in the long-range ordered state. In the spin glass phase, the spin dynamics are strongly  $q$  dependent, suggesting remnant short-range spin correlations. [S0031-9007(99)09306-0]

PACS numbers: 75.40.Gb, 75.10.Nr, 75.50.Bb, 75.50.Lk

One class of disordered ferromagnets shows reentrant spin-glass behavior [1]: magnetization measurements suggest that the materials change from paramagnetic to ferromagnetic (FM) at the Curie temperature  $T_C$ . Upon further lowering the temperature, the spins are progressively frozen below a freezing temperature  $T_f$ . The low temperature spin frozen state is called a reentrant spin glass (SG) or mixed state, in which ferromagnetic order is argued to coexist with spin-glass order [2]. For comparison, in a diluted spin glass, spins freeze directly from a paramagnetic state. Spin waves, the expected collective excitation modes from ferromagnetic long range order, have been studied only at small wave vector,  $Q$ , using inelastic neutron scattering in the FM phase of the reentrant spin glasses FeCr, AuFe, FeAl, NiMn, Fe(Ni,Mn) alloys and amorphous  $(\text{Fe}, T)_{75}\text{P}_{16}\text{B}_5\text{Al}_3$  ( $T = \text{Mn}, \text{Ni}, \text{or Cr}$ ) [3–7]. The spin waves become broad, decrease in energy, and a quasielastic component appears when the temperature approaches  $T_f$ . This short-range quasielastic component continues to increase with lowering temperature in the SG state, as observed in diluted spin glass such as CuMn [8].

Spin glasses are generally associated with large degeneracy of the magnetic states caused by disorder, frustration [9], or both. In a reentrant spin glass, the fact that the FM state occurs at higher temperatures than the SG state suggests a larger entropy for the FM state than for the SG state [1]. This apparent, counterintuitive situation remains a major mystery in the field of disordered magnetic systems [1]. In this work, using a single crystal, we explore spin dynamics in a greatly expanded  $Q$  and  $\omega$  range beyond previous neutron scattering studies [10]. We find that the FM state of the reentrant spin glass  $\text{Fe}_{0.7}\text{Al}_{0.3}$  has a qualitatively different spin dynamics behavior from that of a conventional ferromagnetic state. It consists of a mixture of low energy propagating spin waves at small wave vectors and diffusive paramagnonlike spin fluctuations at large wave vectors. This is strikingly reminiscent of the phonon behavior in structural glasses [11]. This confirms that al-

though there is ferromagnetic order, substantial disorders exist at finite length scales in this anomalous ferromagnetic state. In addition, a strongly  $Q$ -dependent spin excitation spectrum exists in the SG state, suggesting remnant short-range spin correlations. Preliminary results were reported at a conference [12].

The single crystal sample of  $\text{Fe}_{0.7}\text{Al}_{0.3}$  ( $\text{Fe}_{3-\delta}\text{Al}_{1+\delta}$ ,  $\delta = 0.2$ ) used in this study has a volume of  $\sim 1 \text{ cm}^3$  with a mosaic  $\sim 1.5^\circ$ . It has the face-centered-cubic (fcc)  $\text{DO}_3$  structure (space group  $Fm\bar{3}m$ , No. 225) with four crystallographic sites (refer to Fig. 1): the  $\alpha$  sites  $(\frac{1}{4}, \frac{1}{4}, \frac{1}{4})$  and  $(\frac{3}{4}, \frac{3}{4}, \frac{3}{4})$  are occupied only by Fe, the  $\beta$  site  $(\frac{1}{2}, \frac{1}{2}, \frac{1}{2})$  is occupied predominately by Al with minority Fe ( $\sim 9\%$ ), and the  $\gamma$  site (000) is occupied predominately by Fe ( $\sim 70\%$ ) with minority Al [13]. The lattice parameter is  $a = 5.803 \text{ \AA}$  at the room temperature, and there are four formula units in each unit cell. The Curie

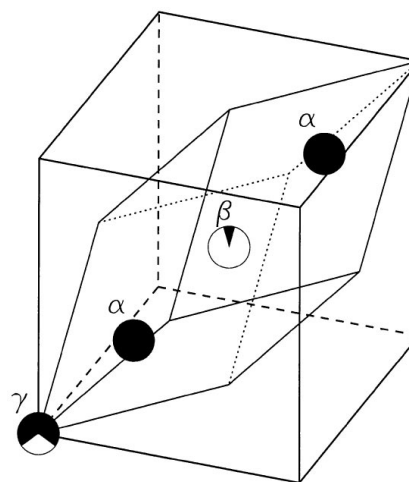


FIG. 1. The fcc lattice structure of  $\text{Fe}_{0.7}\text{Al}_{0.3}$ . Only atoms inside the primitive unit cell are shown. The  $\alpha$  sites are occupied by Fe (black) only. The  $\beta$  site is predominately occupied by Al (white) while the  $\gamma$  site is mostly occupied by Fe.

temperature is  $T_C \approx 520$  K and the spin freezing temperature  $T_f \approx 80$  K [14].

Neutron scattering experiments were performed at the cold neutron triple-axis spectrometers H9A at the High Flux Beam Reactor (HFBR) of BNL, IN12 at ILL Grenoble, thermal neutron triple-axis spectrometers H7 of HFBR, and BT2 at NIST. Pyrolytic graphite (PG) was used as a monochromator and analyzer. A cold beryllium filter was used for cold neutron measurements and a PG filter was used for thermal neutron measurements to reduce higher order neutrons. Spectrometer configurations used in experiments are specified in the figures. The sample was placed inside an aluminum can filled with He exchange gas in a cryostat. It was aligned with the  $(hhl)$  zone coinciding with the scattering plane. We focus in this paper on results from scans along the [111] direction near Bragg points (111) and (000).

The intensity of the magnetic neutron scattering was measured against a flux monitor placed between the sample and the exit collimator for monochromator. It can be expressed [15] as

$$I(\mathbf{Q}, \omega) = Af(k_i) \frac{k_f^3}{\tan\theta_A} |F(\mathbf{Q})|^2 \bar{S}(\mathbf{Q}, \omega), \quad (1)$$

where  $A$  is approximately a constant for a given spectrometer configuration,  $k_i$  and  $k_f$  are, respectively, the initial and final wave number for neutrons,  $2\theta_A$  is the scattering angle for analyzer,  $f(k_i)$  is a correction factor for high order neutrons registered at the flux monitor in a fixed  $k_f$  configuration,  $|F(\mathbf{Q})|^2$  is atomic form factor for Fe, and  $\bar{S}(\mathbf{Q}, \omega)$  is the convolution of the dynamic spin correlation function  $S(\mathbf{Q}, \omega)$  with spectrometer resolution function. The polarization factor for  $\mathbf{Q}$  along [111] has been absorbed in  $A$ . By measuring neutron scattering intensity as a function of momentum transfer  $\hbar\mathbf{Q}$  and energy transfer  $\hbar\omega$ ,  $\bar{S}(\mathbf{Q}, \omega)$  can be directly determined. For the configurations we used, the four-dimensional convolution yields  $\bar{S}(\mathbf{Q}, \omega) \approx S(\mathbf{Q}, \omega)$  for  $|\hbar\omega|$  greater than the energy resolution [16]. Factoring out the thermal occupation factor, the imaginary part of the generalized dynamic magnetic susceptibility is given by

$$\chi''(\mathbf{Q}, \omega) = \pi(1 - e^{-\hbar\omega/k_B T})S(\mathbf{Q}, \omega). \quad (2)$$

The neutron scattering data shown in this paper are normalized to yield either the  $S(\mathbf{Q}, \omega)$  or  $\chi''(\mathbf{Q}, \omega)$ .

We present first our results at 295 K well within the FM phase. Figure 2 shows a few examples of constant  $\mathbf{Q} = (hhh)$  scans near (000). The background (refer to the dashed line) is negligible compared to signal. The resolution limited elastic peak at  $\hbar\omega = 0$  has been studied before [5] and it will not be discussed here. As observed in previous works near the forward direction [3–7],  $S(\mathbf{Q}, \omega)$  peaks at a finite energy. With increasing  $Q$ , the peak energy increases while the damping of the peak becomes stronger. For  $h > 0.06$ , the spectra are overdamped.

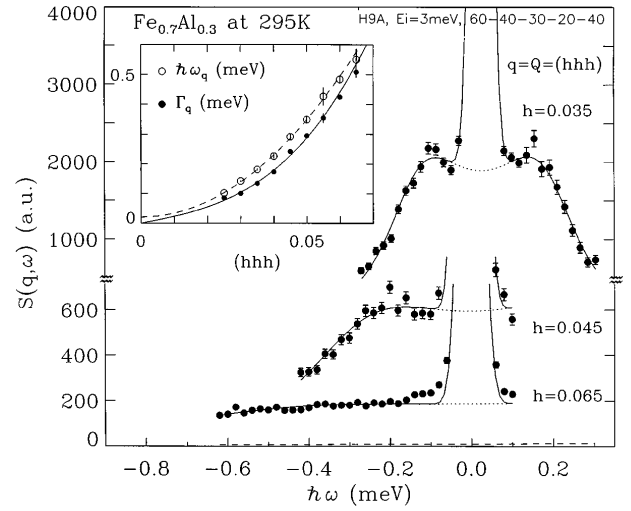


FIG. 2. Small angle inelastic energy scans measured at several  $Q$  values in the FM phase of  $\text{Fe}_{0.7}\text{Al}_{0.3}$ . Inset: Spin wave energy  $\hbar\omega_{\mathbf{q}}$  and damping energy  $\Gamma_{\mathbf{q}}$  [Eq. (3)] vs  $q = (hhh)$ .

We model the magnetic excitations with a form which is equivalent to the damped harmonic oscillator [17]:

$$\chi''(\mathbf{q}, \omega) = C \left( \frac{\Gamma_{\mathbf{q}}}{\hbar^2(\omega - \omega_{\mathbf{q}})^2 + \Gamma_{\mathbf{q}}^2} - \frac{\Gamma_{\mathbf{q}}}{\hbar^2(\omega + \omega_{\mathbf{q}})^2 + \Gamma_{\mathbf{q}}^2} \right), \quad (3)$$

where  $C$  is a constant oscillator strength, and we have chosen  $\mathbf{Q} = \boldsymbol{\tau} + \mathbf{q}$ , where  $\boldsymbol{\tau}$  is the (111) or (000) Bragg point, so that  $\mathbf{q}$  is defined within a Brillouin zone. From a standard least-squares fit to each scan, the energy of the spin wave mode,  $\hbar\omega_{\mathbf{q}}$ , and the damping energy,  $\Gamma_{\mathbf{q}}$ , are obtained (refer to the insert in Fig. 2). The  $\hbar\omega_{\mathbf{q}}$  can be described by

$$\hbar\omega_{\mathbf{q}} = Dq^2 + \Delta \quad (4)$$

with the stiffness constant  $D = 37.4(3)$  meV  $\text{\AA}^2$  and  $\Delta = 0.021(2)$  meV (refer to the dashed line in the inset in Fig. 2). For comparison,  $D = 101$  meV  $\text{\AA}^2$  for stoichiometric  $\text{Fe}_3\text{Al}$ . The value for  $\Delta$  is much smaller than the energy resolution ( $\sim 0.07$  meV) so it may not be significantly different from  $\Delta = 0$ . Even in this propagating spin wave regime, the damping energy,  $\Gamma_{\mathbf{q}}$ , is close to  $\hbar\omega_{\mathbf{q}}$  in magnitude.

The range of energy scans is limited by the energy and momentum conservation conditions

$$-\frac{\hbar^2}{2m}(2k_i Q + Q^2) < \hbar\omega < \frac{\hbar^2}{2m}(2k_i Q - Q^2).$$

For  $Q$  larger than (0.06, 0.06, 0.06) (refer to Fig. 2), the accessible energy range can hardly cover  $\hbar\omega_{\mathbf{q}}$  or  $\Gamma_{\mathbf{q}}$ . To obtain reliable measurement of  $S(\mathbf{q}, \omega)$ , we measure near the Bragg point (111) where a much more extended energy range can be achieved with comparable energy resolution.

An example for  $\mathbf{q} = (0.08, 0.08, 0.08)$  is shown in the inset in Fig. 3. The sharp peak at  $-0.52$  meV does not appear in a similar scan near (000), thus it is not part of the magnetic spectrum we are studying. Its origin is still under investigation. The broad magnetic excitations are now clearly overdamped.

For such overdamped magnetic excitations at large  $q$ , the value for  $\hbar\omega_{\mathbf{q}}$  cannot be obtained reliably. We fixed  $\hbar\omega_{\mathbf{q}}$  according to (4) to estimate  $\Gamma_{\mathbf{q}}$ . The fitting was not very sensitive to  $\hbar\omega_{\mathbf{q}}$ . Values of  $\Gamma_{\mathbf{q}}$  from this and other configurations, spanning more than 2 orders of magnitude in energy, are shown in the main part of Fig. 3 using a log-log scale. Roughly,  $\Gamma_{\mathbf{q}} \propto q^{2.5}$  (the dotted line). However, the  $q$  dependence of  $\Gamma_{\mathbf{q}}$  may be better described by

$$\Gamma_{\mathbf{q}} = \gamma_F q^3 \left[ 1 + \left( \frac{\kappa}{q} \right)^2 \right], \quad (5)$$

with  $\gamma_F = 218(21)$  meV  $\text{\AA}^3$  and an inverse length scale  $\kappa = 0.073(2)$   $\text{\AA}^{-1}$  (refer to the solid line). This  $q$  dependence for damping is very similar to that for paramagnetic spin fluctuations as observed at  $T > T_C$  in ferromagnet MnSi, Pd<sub>2</sub>MnSn, Ni, and Fe [18]. The damping in the ferromagnetic state of Fe<sub>0.7</sub>Al<sub>0.3</sub>, thus, appears to share the same characteristics with damping in the thermally disordered paramagnetic state of ferromagnets.

To better appreciate this unusual magnetic excitation spectrum, intensity contours of  $S(\mathbf{q}, \omega)$  for Fe<sub>0.7</sub>Al<sub>0.3</sub> at 295 K, using Eqs. (2) and (3) and experimentally determined  $\omega_{\mathbf{q}}$  and  $\Gamma_{\mathbf{q}}$  in (4) and (5), are shown in Fig. 4. There exists a critical wave number,  $q_0$ , where  $\hbar\omega_{q_0} = \Gamma_{q_0}$ . At room temperature,

$$q_0 \approx \frac{D}{2\gamma_F} \left( 1 + \sqrt{1 - \left( \frac{2\gamma_F \kappa}{D} \right)^2} \right) \\ = 0.13 \text{ \AA}^{-1} = 0.07 \text{ rlu}. \quad (6)$$

For  $q < q_0$ ,  $\Gamma_{\mathbf{q}} < \hbar\omega_{\mathbf{q}}$ . A constant- $q$  scan yields a peak at a finite energy (c.f. Fig. 2), demonstrating that damped but still propagating spin waves exist. For  $q > q_0$ ,  $\Gamma_{\mathbf{q}} > \hbar\omega_{\mathbf{q}}$  and the spin excitation spectrum becomes overdamped (c.f. inset in Fig. 3). The spectrum in this part of phase space is reminiscent of the paramagnon spectrum of conventional ferromagnetic materials at  $T > T_C$  [18]. Specifically, while a constant- $q$  scan cutting through  $S(\mathbf{q}, \omega)$  yields no peak at a finite energy, a constant- $\hbar\omega$  scan shows a peak at finite  $q$ . Some examples of such constant- $\hbar\omega$  scans for Fe<sub>0.7</sub>Al<sub>0.3</sub> are shown in Fig. 5. It is interesting to note that a crossover at finite  $Q$  from propagating to diffusive vibrational modes exists in structural glasses [11].

One source of damping is interactions between spin waves [19]. However, at  $T = 295$  K  $\approx 0.6T_C$ , they would not overdamp spin waves at a very small wave vector  $q \approx (0.07, 0.07, 0.07) = 0.14q_{\text{BZ}}$ , where  $q_{\text{BZ}} = (\frac{1}{2}, \frac{1}{2}, \frac{1}{2})$  is the Brillouin zone boundary. Furthermore, damping due to spin wave interactions approaches zero when  $T \rightarrow 0$ , while in Fe<sub>0.7</sub>Al<sub>0.3</sub> damping increases upon cooling [5]. Therefore, spin wave interactions are not the main cause of damping in Fe<sub>0.7</sub>Al<sub>0.3</sub>. Strong damping in this material is most likely due to disorder introduced by a random mixture of Fe and Al at the  $\gamma$  and  $\beta$  sites, which at  $T_f$  also freezes the spins.

Finally, we compare magnetic excitations at 294 K in the FM phase to those at 18 K in the SG phase. To facilitate such a comparison, data are presented as  $\chi''(\mathbf{q}, \omega)$  in Fig. 5 to remove the thermal occupation factor [Eq. (2)]. Spin waves at small  $Q$  near  $\tau = (000)$  are known to become overdamped at low temperatures from previous cold neutron studies [3–7]. This fact remains true near the Bragg point (111) [16] and is reflected in the enhanced

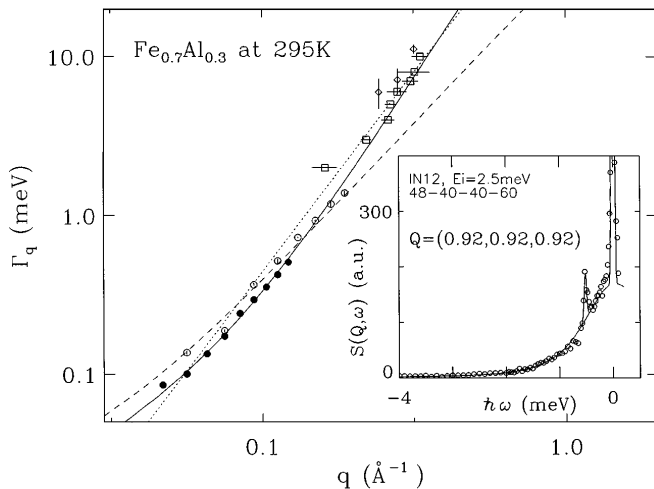


FIG. 3. Damping energy  $\Gamma_{\mathbf{q}}$  vs  $q$ . The solid line is a fit to Eq. (5) and the dotted line is  $\Gamma_{\mathbf{q}} \propto q^{2.5}$ . The solid circles are from measurements near (000) at H9A with fixed  $E_i = 3$  meV and horizontal collimations  $60^\circ\text{-}40^\circ\text{-}30^\circ\text{-}20^\circ\text{-}40^\circ$ ; the open circles near (111) at IN12 with  $E_i = 2.5$  meV and  $48^\circ\text{-}40^\circ\text{-}40^\circ\text{-}60^\circ$ ; the squares near (111) at H7 with  $E_f = 14.7$  meV and  $40^\circ\text{-}20^\circ\text{-}40^\circ\text{-}40^\circ$ ; and the diamonds near (111) at BT2 with  $E_f = 14.7$  meV and  $60^\circ\text{-}20^\circ\text{-}20^\circ\text{-}80^\circ$ . The dashed line is  $\hbar\omega_{\mathbf{q}}$  [Eq. (4)] for reference. Inset: A constant- $Q$  scan [ $q = (0.08, 0.08, 0.08)$ ] near (111) measured in the FM phase.

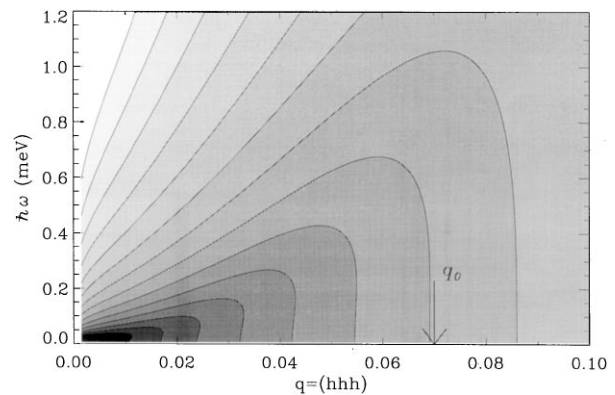


FIG. 4. Intensity contour of  $S(\mathbf{q}, \omega)$  in units of  $C \times \text{meV}$  [refer to Eq. (3)] using the experimentally determined  $\omega_{\mathbf{q}}$  and  $\Gamma_{\mathbf{q}}$  measured at 295 K. Each fading contour level designates a decrease of 1 order of magnitude. The arrow indicates the critical wave vector.

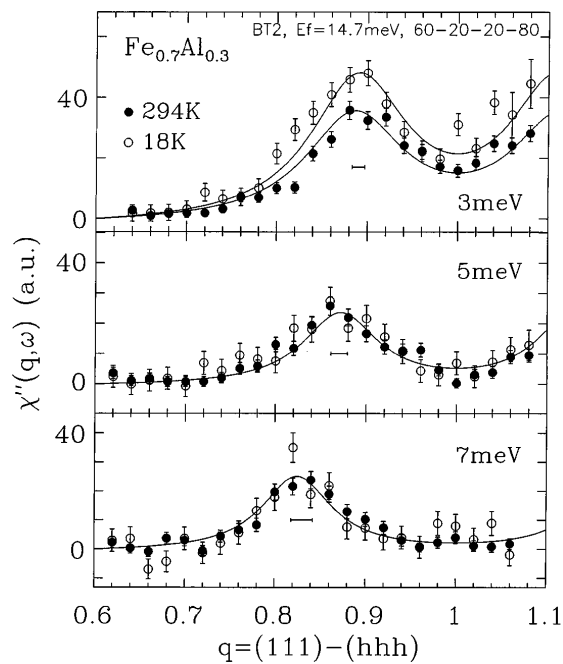


FIG. 5.  $\chi''(\mathbf{q}, \omega)$  determined from constant- $E$  scans for  $\hbar\omega = 3, 5,$  and  $7$  meV. The solid circles were measured at 294 K in the FM phase, and the open circles at 18 K in the SG phase. The horizontal bars indicate the full width at half maximum of the projected instrument resolution function.

intensity in the SG state (refer to the open circles) for the  $\hbar\omega = 3$  meV scans in Fig. 5. The prevailing view about the diffuse magnetic fluctuations is that frozen spins undergo uncorrelated relaxations. However, unexpectedly, the strong  $q$ -dependent structure of  $\chi''(\mathbf{q}, \omega)$  in the FM state remains in the SG state. In fact, the  $\chi''(\mathbf{q}, \omega)$  is identical at 18 K and at 295 K for  $\hbar\omega \geq 5$  meV. It appears that changes in the dynamic magnetic spectrum in Fig. 4 upon reaching the SG state occur mainly as a result of  $q_0$  decreasing with temperature, so that when  $T$  approaches zero, spectral weight at small  $q$  and  $\omega$  builds up and no propagating features are present. The paramagnon-like spectrum now covers the entire  $q$ - $\omega$  space, indicating remnant short-range spin clusters. It is interesting to note that the SG state with frozen disorder exhibits similar spin dynamics as the conventional paramagnetic state where dynamic disorder is caused by thermal energy.

In conclusion, we have characterized over a large  $\omega$  and  $\mathbf{q}$  range the anomalous spin dynamics in the FM phase of the reentrant spin glass material  $\text{Fe}_{0.7}\text{Al}_{0.3}$ . Like the SG state, the FM state seems also to be a mixed state. In this case, ferromagnetic order and paramagneticlike disorder coexist at different length scales. In the SG state, the paramagnonlike spin excitations dominate spin dynamics, suggesting short-range spin clusters. This picture, from our experiment, now indicates that the so-called FM state can possess a larger entropy. It offers a new direction in solving the reentrant spin-glass paradox.

We thank P. Böni, G. Shirane, R. A. Cowley, J. D. Axe, J. Tranquada, and A. Zheludev for useful discussions;

J. W. Lynn, S.-H. Lee, and I. Zalitznyak for hospitality at NIST. The work at BNL was supported by DOE under Contract No. DE-AC02-98CH10886 and in part by the U.S.-Japan program on Neutron Scattering, at LANL under the auspices of DOE.

- [1] J. A. Mydosh, *Spin Glasses: An Experimental Introduction* (Taylor & Francis, London, 1993); K. Binder and A. P. Young, *Rev. Mod. Phys.* **58**, 801 (1986); M. J. P. Gingras, in *Magnetic Systems with Competing Interactions*, edited by H. T. Giep (World Scientific, Singapore, 1994).
- [2] M. Gabay and G. Toulouse, *Phys. Rev. Lett.* **47**, 201 (1981); D. M. Cragg, D. Sherrington, and M. Gabay, *ibid.* **49**, 158 (1982); M. A. Moore and A. J. Brag, *J. Phys. C* **15**, L301 (1982).
- [3] C. R. Fincher, Jr., S. M. Shapiro, A. C. Palumbo, and R. D. Parks, *Phys. Rev. Lett.* **45**, 474 (1980); S. M. Shapiro, C. R. Fincher, Jr., A. C. Palumbo, and R. D. Parks, *Phys. Rev. B* **24**, 6661 (1981).
- [4] A. P. Murani, *Phys. Rev. B* **28**, 432 (1983).
- [5] K. Motoya, S. M. Shapiro, and Y. Muraoka, *Phys. Rev. B* **28**, 6183 (1983); K. Motoya and Y. Muraoka, *J. Phys. Soc. Jpn.* **62**, 2819 (1993).
- [6] G. Aeppli, S. M. Shapiro, R. J. Birgeneau, and H. S. Chen, *Phys. Rev. B* **29**, 2589 (1984); R. W. Erwin, J. W. Lynn, J. J. Rhyne, and H. S. Chen, *J. Appl. Phys.* **57**, 3473 (1985); J. P. Wicksted, S. M. Shapiro, and H. S. Chen, *ibid.* **55**, 1697 (1984).
- [7] S. Lequien, B. Hennion, and S. M. Shapiro, *Phys. Rev. B* **38**, 2669 (1988); M. Hennion, B. Hennion, I. Mirebeau, and S. Lequien, *J. Appl. Phys.* **63**, 4071 (1988).
- [8] A. P. Murani and J. L. Tholence, *Solid State Commun.* **22**, 25 (1977); F. Mezei and A. P. Murani, *J. Magn. Mater.* **14**, 211 (1979); Y. J. Uemura *et al.*, *Phys. Rev. B* **31**, 546 (1985).
- [9] A. P. Ramirez, *Annu. Rev. Mater. Sci.* **24**, 453 (1994); S.-H. Lee *et al.*, *Europhys. Lett.* **35**, 127 (1996).
- [10] S. M. Shapiro, in *Spin Waves and Magnetic Excitations*, edited by A. S. Borovik-Romanov and S. K. Sinha (Elsevier, Amsterdam, 1988).
- [11] M. Foret *et al.*, *Phys. Rev. Lett.* **77**, 3831 (1996); **81**, 2100 (1998).
- [12] S. Raymond *et al.*, *Physica (Amsterdam)* **241B-243B**, 597 (1998).
- [13] J. W. Cable, L. David, and R. Parra, *Phys. Rev. B* **16**, 1132 (1977).
- [14] R. D. Shull, H. Okamoto, and P. A. Beck, *Solid State Commun.* **20**, 863 (1976).
- [15] N. J. Chesser and J. D. Axe, *Acta Cryst. A* **29**, 160 (1973).
- [16] W. Bao *et al.* (to be published).
- [17] R. A. Cowley, W. J. Buyers, P. Martel, and R. W. H. Stevenson, *J. Phys. C* **6**, 2997 (1973).
- [18] Y. Ishikawa *et al.*, *Phys. Rev. B* **31**, 5884 (1985); O. W. Dietrich, J. Als-Nielsen, and L. Passell, *ibid.* **14**, 4923 (1976); J. P. Wicksted, P. Böni, and G. Shirane, *ibid.* **30**, 3655 (1984); G. Shirane, O. Steinsvoll, Y. J. Uemura, and J. Wicksted, *J. Appl. Phys.* **55**, 1887 (1984).
- [19] W. Marshall, E. Balcar, and S. W. Lovesey, *Commun. Solid State Phys.* **2**, 204 (1970).